Active Piezoelectric Energy Harvesting: General Principle and Experimental Demonstration

YIMING LIU, GENG TIAN, YONG WANG, JUNHONG LIN, QIMING ZHANG AND HEATH F. HOFMANN*

Department of Electrical Engineering, The Pennsylvania State University, 121 Electrical Engineering East University Park, PA 16802, USA

ABSTRACT: In piezoelectric energy harvesting systems, the energy harvesting circuit is the interface between a piezoelectric device and an electrical load. A conventional view of this interface is based on impedance matching concepts. In fact, an energy harvesting circuit can also apply electrical boundary conditions, such as voltage and charge, to the piezoelectric device for each energy conversion cycle. An optimized electrical boundary condition can therefore increase the mechanical energy flow into the device and the energy conversion efficiency of the device. We present a study of active energy harvesting, a type of energy harvesting approach which uses switch-mode power electronics to control the voltage and/or charge on a piezoelectric device relative to the mechanical input for optimized energy conversion. Under quasi-static assumptions, a model based on the electromechanical boundary conditions is established. Some practical limiting factors of active energy harvesting, due to device limitations and the efficiency of the power electronic circuitry, are discussed. In the experimental part of the article, active energy harvesting is demonstrated with a multilayer PVDF polymer device. In these experiments, the active energy harvesting approach increased the harvested energy by a factor of five for the same mechanical displacement compared to an optimized diode rectifier-based circuit.

Key Words: energy harvesting, piezoelectric devices, power electronics, power scavenging.

INTRODUCTION

THE generation of electrical power from mechanical motion and structural vibrations is an active area of interest, made practical by the reduced power consumption of electronic systems. The ability to harvest electrical energy from the ambient environment has enabled new technologies, such as self-powering wireless sensor networks. Piezoelectric devices have been a popular means of achieving electromechanical energy conversion in these applications, due to the ease in which these devices can be incorporated into mechanical structures and their relative simplicity when compared to magnetic field-based generators. A key aspect of an energy harvesting system is the power electronic circuitry, which interfaces the piezoelectric device with the electronic load, as a well-designed circuit can increase the amount of energy harvested. Many different circuit topologies have been proposed to achieve this function. These circuits can be characterized as 'passive' circuits such as diode rectifier circuits (Ottman et al., 2002, 2003), or 'semi-active' circuits that open or close a switch when the peak force is achieved across the device (Smalser, 1997; Richard et al., 2000; Badel, 2005; Badel et al., 2005, 2006; Faiz et al., 2005; Lefeuvre et al., 2005). Semi-active circuits have been shown to provide more power than passive circuits. However, these circuits utilize passive components, such as inductors, that determine the transient behavior of the device when the switch is open or closed. In contrast, active energy harvesting utilizes a bidirectional switch-mode converter to control the voltage or charge on the electrodes of a piezoelectric device. Advantages over other approaches are a greater degree of control over the voltage or current waveforms of the piezoelectric device. For example, in synchronized switched harvesting on inductor (SSHI) circuits (Badel et al., 2006), the peak current seen by the piezoelectric device during voltage transitions is determined by the inductor used in the circuit. High-peak currents during this transition can increase the losses in the circuit. These peak currents can be reduced by the use of a larger inductance, but this can be practically difficult in certain applications due to the required size of the inductor, and the additional resistance that accompanies a larger inductance for a

*Author to whom correspondence should be addressed.
E-mail: hofmann@engr.psu.edu
Figures 8–10 and 12–15 appear in color online: http://jim.sagepub.com

1045-389X/09/05 0575–11 $10.00/0 DOI: 10.1177/1045389X08098195

given size. In active energy harvesting techniques, the peak current through the piezoelectric device can be limited through proper control of the power electronic converter.

The basic circuit configuration of active energy harvesting was first patented by Hagood and Ghandi (2003), in which a bidirectional converter directly drives a piezoelectric device. This patent, however, did not discuss appropriate electrical boundary conditions to apply to the device. In Liu et al. (2005), appropriate boundary conditions for an electrostrictive device were discussed. In this article, the subject will be appropriate boundary conditions for a piezoelectric device. This article will show that, with active energy harvesting, the amount of energy that can potentially be harvested is limited only by the electrical and mechanical limitations of the piezoelectric device, and the electrical limitations and efficiency of the power electronic circuitry.

QUASI-STATIC MODEL OF PIEZOELECTRIC DEVICE

Piezoelectric Device

Piezoelectricity is a mutual coupling between mechanical strain/stress and electrical field/charge, and can be described by the following linear constitutive equations (IEEE Standard on Piezoelectricity, 1988):

$$\begin{aligned} S_{ij} &= s^E_{ijkl} T_{kl} + d_{ijm} E_m, \\ D_n &= d_{nkl} T_{kl} + \varepsilon^T_{mn} E_m, \end{aligned} \tag{1}$$

where S_{ij} and T_{kl} are the mechanical strain and stress tensors, and D_n and E_m are the electric displacement and field vectors, respectively. In (1) the Einstein summation convention is used. Monolithic piezoelectric materials are rarely used as standalone devices, as the generated strain of a piezoelectric material is small (usually <0.1% for ceramics), even under high field. Piezoelectric materials, especially ceramics such as PZT, are relatively stiff and require a large stress to be effectively strained. They are therefore often embedded into mechanical structures, constituting devices. Those structures include unimorph/bimorph cantilever beams (Wang et al., 1999), matrix composite structures, and cymbal structures (Newnham and Zhang, 2001). Piezoelectric materials themselves are also often laminated into multilayer structures, or made into fibers to further reduce voltage levels or enhance their robustness (Newnham et al., 1978). Although the constitutive equations of piezoelectricity are in tensor form, a piezoelectric device can often be described by scalar equations. Under the quasi-static assumption, which neglects the dynamic behavior at the resonance of the device, linear, frequency-independent equations that represent the device are written as follows:

$$\begin{aligned} \delta &= s^V F + dV, \\ Q &= dF + C^F V, \end{aligned} \tag{2}$$

where δ is the deflection or displacement of the device, Q is the electrical charge on the electrodes of the device, F is the force exerted on the device, V is the voltage across the electrodes, s^V is the compliance under constant voltage, d is the general piezoelectric coefficient, and C^F is the capacitance under constant force. The chosen model of the device is based on the quasi-static assumption, as it reveals the fundamentals of piezoelectric energy conversion without overly complex mathematic derivation. Such a model is useful for applications where the frequency of excitation is lower than the mechanical resonance of the device. It is also worth noting that this model does not take into account power loss within the device.

Boundary Condition Integration Model

The piezoelectric energy conversion process can be graphically presented in the force–displacement and voltage–charge planes illustrated in Figure 1. An energy conversion cycle is the enclosed mechanical and electrical path the device traverses during one period of mechanical excitation. The enclosed area of the electrical path is calculated as follows:

$$W_e = \oint V \, \mathrm{d}Q = \int_0^T Vi \, \mathrm{d}t. \tag{3}$$

Integration of (3) yields time integration of the instantaneous electrical power, which represents the total converted electrical energy over a period. Similarly, it can be shown that the enclosed area in the mechanical domain:

$$W_m = \oint F \, \mathrm{d}\delta \tag{4}$$

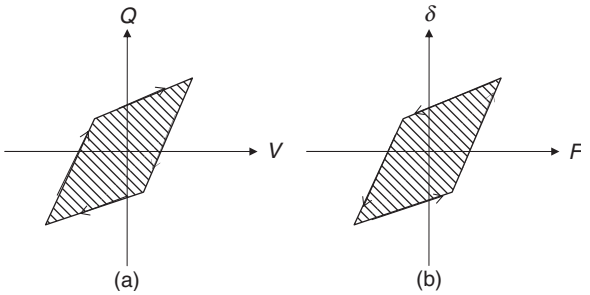

Figure 1. *Illustration of energy harvesting cycle: (a) electrical domain where shaded area represents the converted electrical energy during one cycle; (b) mechanical domain where shaded area represents input mechanical energy for one cycle.*

represents the mechanical energy that is converted to electrical energy. If losses in the device are ignored, this mechanical energy is always equal to the output electrical energy. In other words, the two enclosed areas in both domains are equal, though of different shapes. Equation (4) also provides intuition into the active energy harvesting approach. In the case of a non-electroactive material, this integration would be zero. However, in the case of a piezoelectric device, the displacement of the device can be adjusted electrically. Hence, for a given mechanical force F, the displacement δ and the integrated area in Equation (4) can be increased electrically, and hence the amount of mechanical energy to be converted can be increased as well. It is this ability to control the amount of mechanical energy in the device that is converted to electrical energy that makes the active approach so attractive. In the following analysis, we will assume that the mechanical force applied to the device has a peak-to-peak value F_L that remains constant regardless of the electrical excitation. These assumptions are valid for some applications, such as power-generating shoes, in which the amplitude of the applied force mostly depends on the body weight of the person. Provided the electrical boundary conditions are changed sufficiently slowly, the force on the device due to body weight should not be affected. Furthermore, the frequency of excitation associated with walking is sufficiently low to avoid the excitation of any mechanical resonances associated with the device. It should be noted that the principles of active energy harvesting can also be applied to other forms of excitation.

The assumption of a mechanical force excitation that is independent of the other states of the device allows for a simplistic circuit model, shown in Figure 2. The model consists of the electrode capacitance in parallel with a current source $I_p(t)$, whose value is proportional to the negative of the derivative of the applied force.

ACTIVE ENERGY HARVESTING

Quasistatic Energy Harvesting Cycles

Active energy harvesting is a technique that can push energy harvesting to the limits of the piezoelectric device, the power electronic circuitry, or the mechanical structure. Examples are voltage limitations due to electrical fields that cause breakdown or depoling of the piezoelectric material, or the voltage capabilities of the power electronic circuitry. In the following we will use the subscript 'L' to denote limits to the piezoelectric mechanical and electrical variables due to device properties or external conditions. These limits will be given in this article in terms of peak-to-peak values. In the following sections, we will analyze the maximum energy that can be harvested by the piezoelectric device under various combinations of mechanical and electrical limitations.

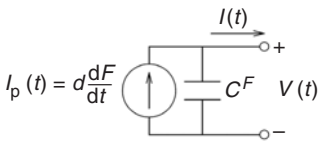

Figure 2. *Circuit model for piezoelectric device with independent force excitation.*

DIODE RECTIFIER CIRCUIT

In order to gauge the benefits of active energy harvesting, we will first analyze the energy harvesting trajectory of the (passive) diode rectifier circuit, a common component in energy harvesting circuits. The full-bridge rectifier circuit is shown in Figure 3.

The resulting trajectories are shown in Figure 4.

Suppose the mechanical excitation exerted on the device is a force with a fixed peak-to-peak amplitude F_L. In trajectories 1–2 and 3–4, the rectifier is reverse biased and the device is therefore in an open-circuit condition, and so the electrical charge across the device is constant. Hence in the electrical plot these trajectories are horizontal paths. In trajectories 2–3 and 4–1, the diodes are forward biased, so the voltage on the device is equal to the DC output voltage of the rectifier, V_{dc}, which can be assumed to be constant if the output capacitance of the rectifier is sufficiently large. These paths are vertical in the electrical domain. The force F_r at which the device

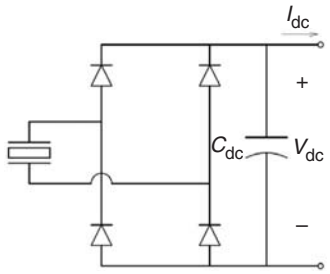

Figure 3. *Passive energy harvesting using full-bridge diode rectifier.*

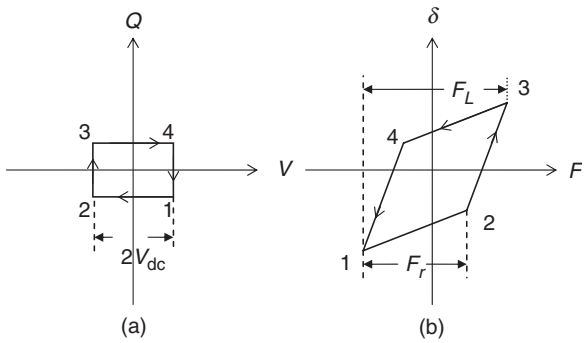

Figure 4. *Energy harvesting cycle of piezoelectric device connected to full-bridge diode rectifier circuit.*

generates an open-circuit voltage equal to the DC output voltage is as follows:

$$F_r = \frac{2C^F}{d} V_{\mathrm{dc}}. \tag{5}$$

The energy converted in one cycle is equal to the enclosed rectangular area in the electrical domain:

$$W = 2d\left(F_L - \frac{2C^F}{d} V_{\mathrm{dc}}\right) V_{\mathrm{dc}}. \tag{6}$$

This energy is a function of the DC output voltage and it maximizes when:

$$V_{\mathrm{dc}} = \frac{1}{4}\frac{dF_L}{C^F} = \frac{1}{4} V_{\mathrm{oc}}, \tag{7}$$

where V_{oc} corresponds to the peak-to-peak open-circuit voltage of the device generated by the mechanical excitation, i.e.,

$$V_{\mathrm{oc}} = \frac{dF_L}{C^F}. \tag{8}$$

The energy harvested from the device under these conditions is:

$$W_{\mathrm{max\ rect}} = \frac{d^2F_L^2}{4C^F} = \frac{1}{4} C^F V_{\mathrm{oc}}^2. \tag{9}$$

ACTIVE ENERGY HARVESTING

In this section, we will investigate a type of active energy harvesting involving the control of the voltage across the device. An example of a power electronic circuit that can accomplish this task is a full-bridge inverter, shown in Figure 5. The MOSFETs in this circuit are operated in 'switch-mode' (i.e., they are considered as ideal switches that are either 'on' or 'off'). Through the use of pulse-width modulation (PWM) techniques, the full-bridge inverter can apply an average-value voltage across the device that can vary between $\pm V_{\mathrm{dc}}$, where V_{dc} is a constant DC voltage that can be either a battery voltage, or a voltage across a large capacitance (Mohan et al., 2003). The inductance L is present to filter the pulse-width modulated voltage so that the piezoelectric device does not experience instantaneous voltage transitions. The rate of change of the voltage across the device, and hence the magnitude of the device current due to the electrode capacitance, is therefore controlled by the PWM.

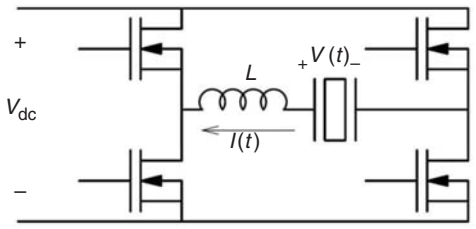

Figure 5. *Full-bridge inverter circuit for active energy harvesting.*

In the presented approach, the voltage across the device is transitioned between a maximum value $V_{\max}$ and a minimum value $V_{\min}$, at the peak values of the applied force, as shown in Figure 6. In trajectories 1–2 and 3–4, the voltage across the device is kept at a constant value by the power electronic circuit while the applied force changes between its minimum and maximum values. In trajectories 2–3 and 4–1, the power electronic circuitry changes the voltage between its maximum and minimum values when the applied force is at its extrema.

The converted energy is calculated from the area of either parallelogram in the electrical or mechanical domain in Figure 6:

$$W_{\mathrm{ac}} = dF_L(V_{\max} - V_{\min}) = dF_L V_L = C^F V_{\mathrm{oc}} V_L. \tag{10}$$

The force, voltage, and current time waveforms of an active energy harvesting cycle are shown in Figure 7. In this particular case the force excitation is sinusoidal, and the voltage is transitioned between positive and negative force values of the same magnitude. When the

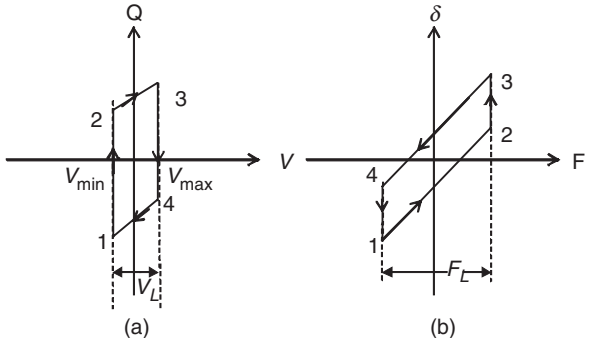

Figure 6. *Active energy harvesting.*

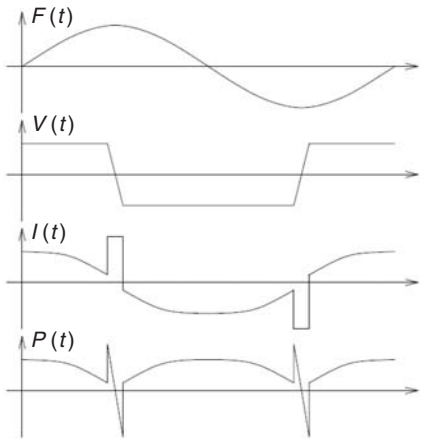

Figure 7. *Waveforms of active energy harvesting with sinusoidal applied force.*

voltage across the device is kept constant, there is no capacitive current and the output current of the device $I(t)$ is equal to that of the piezoelectric current $I_p(t)$. The sign of this current matches that of the voltage, resulting in electrical power $P(t) = V(t)I(t)$ removed from the device. During the voltage transitions the derivative of the force, and hence the piezoelectric current, is essentially zero. The power flow under these conditions is therefore associated with the discharging and charging of the electrode capacitance. When discharging the capacitance, electrical power is once again removed from the device. However, electrical power must flow into the device when charging the electrode capacitance.

COMPARISON OF ACTIVE ENERGY HARVESTING TO DIODE RECTIFIER CIRCUIT

From Equations (9) and (10) it can be seen that the maximum energy that can be harvested from the rectifier circuit is a function of only the applied force, whereas in the case of active control it is a function of the force and the applied voltage. Hence, theoretically, in the case of active control and the assumption of an independent mechanical force excitation, the amount of harvested energy can be increased arbitrarily high by increasing the magnitude of the peak-to-peak voltage applied to the terminals of the device. In practice, however, the amount of energy harvested will be constrained by the electrical and mechanical limitations of the device. For example, the depoling and breakdown fields of the piezoelectric material will limit the voltage that can be applied to the device. As we will see in the next section, the amount of energy that can be harvested is also a function of the efficiency of the power electronics driving the device. Furthermore, the assumption of a force excitation that is independent of the device state may also become questionable when the electrically induced displacement of the device becomes large.

Efficiency of Power Electronics

The active energy harvesting trajectories shown in the prequel require bidirectional power flow through the electrical terminals of the device, and hence through the power electronic circuitry driving the device, due to the need to charge the electrode capacitance. As a result, the efficiency of the power electronic circuitry will affect the maximum amount of energy that can be harvested. The efficiency of the circuitry is defined as follows:

$$\eta = \frac{\text{Output Energy/Cycle}}{\text{Input Energy/Cycle}} = 1 - \frac{\text{Loss/Cycle}}{\text{Input Energy/Cycle}}. \tag{11}$$

The net energy harvested by the energy harvesting system is therefore the total energy extracted from the system, ηW_{out}, minus the total energy put into the system, $(1/\eta)W_{in}$. This is represented mathematically as follows:

$$W_{net} = \eta W_{out} - \frac{1}{\eta} W_{in}. \tag{12}$$

During a single cycle, the energy flowing between the electrical terminals of the device and the circuit consists of electromechanically converted energy and energy stored in the electrode capacitance. The direction and amount of energy flow depends upon the signs of the voltages applied to the device. Without loss of generality, we will assume $V_{max} > 0$, and consider two cases:

(1) Case 1: $V_{min} \geq 0$

Under these conditions, it can be shown that the total input electrical energy to the device is given by:

$$W_{in} = dF_L V_{min} + \frac{1}{2} C^F \left(V_{max}^2 - V_{min}^2\right), \tag{13}$$

and the output energy is:

$$W_{out} = dF_L V_{max} + \frac{1}{2} C^F \left(V_{max}^2 - V_{min}^2\right). \tag{14}$$

(2) Case 2: $V_{min} < 0$

When V_{min} is negative, the input energy can be shown to be:

$$W_{in} = \frac{1}{2} C^F \left(V_{max}^2 + V_{min}^2\right), \tag{15}$$

and the output energy is given by:

$$W_{out} = d(V_{max} - V_{min})F_L + \frac{1}{2} C^F \left(V_{max}^2 + V_{min}^2\right). \tag{16}$$

When comparing the two cases, it can be seen that the amount of oscillating energy in the cycle is minimized if Case 2 is chosen, and:

$$V_{min} = -\frac{V_L}{2}, \quad V_{max} = \frac{V_L}{2}. \tag{17}$$

Under these conditions, the net energy is given by:

$$W_{net} = C^F \left[\eta V_{oc} V_L - \frac{1}{4}\left(\frac{1}{\eta} - \eta\right) V_L^2\right]. \tag{18}$$

Inspection of this expression reveals that the net energy can be optimized through appropriate choice of V_L. This optimal value is given by:

$$V_L = 2\left(\frac{\eta^2}{1 - \eta^2}\right) V_{oc}. \tag{19}$$

At this voltage level, the maximum energy harvested is given by:

$$W_{\max\ ac} = \left(\frac{\eta^3}{1-\eta^2}\right) C^F V_{oc}^2. \qquad (20)$$

The above function is very sensitive to the power electronic efficiency η, especially when it is high, as shown in Figure 8 where the energy harvested is compared to that of the diode rectifier circuit. We note that the expression for the rectifier circuit does not take into account the efficiency of the rectifier, and hence these results are conservative. A detailed derivation of Equation (20) is provided in an appendix. The efficiency of power electronic converters often varies from 70% to as high as 95%.

EXPERIMENTAL RESULTS

Piezoelectric Device

In the experiment presented in this article, a commercial PVDF film (from Measurement Specialties, Inc.) was used for the piezoelectric material. The thickness of the material used was 2 μm. The film was uniaxially stretched and corona-poled by the manufacturer. The properties of this film are provided in Table 1. This material has been demonstrated to withstand high strain (~3%) without degrading the piezoelectric responses under quasi-static conditions (Wang et al., 2007).

The PVDF film was then cut into rectangular pieces of 25 cm × 4.2 cm, with the long dimension (25 cm) along the film stretching direction. Large-area aluminum electrodes were deposited by a Semicore® e-beam evaporator on both sides with an effective area of 20 cm × 4 cm. In order to make the electrodes adhere well to the polymer film, the film surface was cleaned with IPA in a clean room environment before Al was deposited.

Since it is difficult to make large-volume piezoelectric devices using a single-layer film, multilayer films were made to fabricate the piezoelectric device. There is another advantage to using multilayer piezoelectric films instead of single layer film, as this increases the total capacitance and piezoelectric constant of the device while maintaining the same open-circuit output voltage as a single-layer film. After aluminum electrodes were deposited, the films were bound together using INSULGEL® 50 soft epoxy gel. Because this gel is very soft even after it is cured, the clamping effect from the epoxy layer during vibration will be very small and can be neglected. The electrodes of different layers were connected and bound with conductive wire and silver glue.

Due to the internal polarization direction of PVDF, improper connections among the electrodes of multilayer films may degrade or even shut down the output voltage and power. Before the films were bound together, each film polarization was checked by using a d_{33} meter, and the polarization direction was marked on the margin place of each film. All the electrodes were electrically connected as positive-to-positive, negative-to-negative. In order to make it convenient during testing, the lead electrodes were arranged at the same end of the film. The Al electrodes were deposited as shown in Figure 9. Two types of electrodes were made during deposition. These structures make it easy to bind the positive-to-positive and negative-to-negative, and to put the same-polarity electrodes at the same side of the films, as shown in Figure 9.

Mechanical Testing System

A computer programmable material testing system (Instron Model 1331) was used in the following

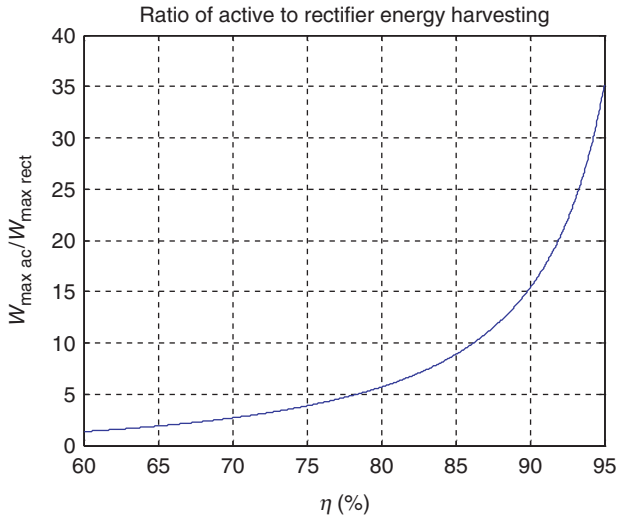

Figure 8. *The performance of active energy harvesting compared to the diode rectifier circuit as function of the efficiency of the power electronic circuitry.*

Table 1. Properties of PVDF film under quasi-static conditions.

	d_{31} (pC/N)	ε_{33} (ε_0)	Y (GPa)	k_{31}
24 μm PVDF	21	11.6	2.9	0.11

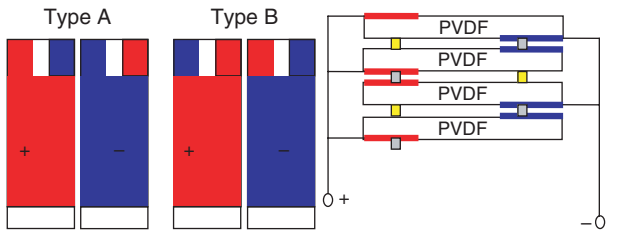

Figure 9. *Left: electrode shape (top view). Right: multilayer films (cross-section view).*

experiments to apply a sinusoidal displacement with constant offset to the piezoelectric device. Soft plastic bars are used as the sample holders for their high electrical insulation abilities. Below the device a universal joint was inserted beneath the sample holder to achieve a uniform pressure on the device. In order to satisfy the quasi-static assumption, the mechanical force frequency was set to 5 Hz, low enough so that no mechanical resonance is excited in the device. The experimental setup is shown in Figure 10.

Power Electronic Circuitry

The core circuit of the active approach is composed of a bidirectional full-bridge converter as the interface between the piezoelectric device and a high-voltage bus, as shown in Figure 11. The switches in the inverter are IXSYS IXTY01N100m MOSFETs, each rated at 1000 V and 100 mA. A controllable DC voltage source provides the bus voltage for the circuit. A DC load resistance $R_{load} = 100\,k\Omega$ is connected across the DC bus. Shunt resistors $R_{sense1} = R_{sense2} = 1\,k\Omega$ are used to measure the currents through the load resistance and from the voltage source, respectively.

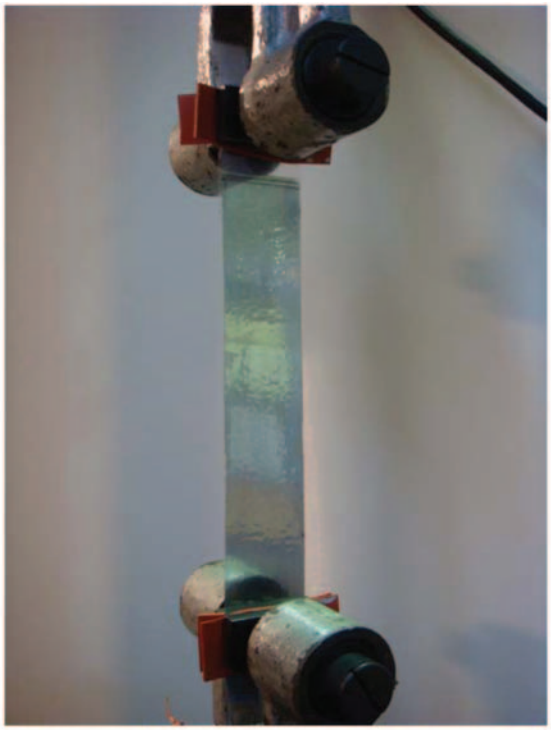

Figure 10. *PVDF sample excited by Instron Model 1331 materials testing system.*

The active controller is implemented using a dSpace DS1104 controller board. The board includes a Texas Instruments TMS320C32 floating-point digital signal processor (DSP), analog-to-digital (ADC) converters for sampling measurements, and pulse-width modulated (PWM) signal outputs for controlling the converter. The control algorithm was developed in MATLAB using the graphical interface Simulink and the Real-Time Workshop to generate the controller code for the DSP. The controller is composed of four major parts, as shown in Figure 11. First, an analog/digital converter is implemented which is used to sample the measured displacement of the piezoelectric device (provided by the materials testing system). This measured displacement is then fed into a phase-locked loop, which is used to generate a pure sinusoidal waveform in phase with the sampled displacement. This signal is then fed into a peak detector, which activates a PWM signal generator to enable a voltage transition across the piezoelectric device. In order to reduce switching losses, which can significantly reduce the performance of the active approach, the controller pulse-width modulates only one of the low-side MOSFETs at a time, depending upon whether the voltage across the device is being increased or decreased. The corresponding upper switch is only closed when the piezoelectric capacitance is being charged; otherwise, both of the upper switches are open. A high-impedance isolated voltage probe was used to measure the voltage across the piezoelectric device, and a Tektronix AM503B current probe was used to measure the terminal current of the device. Thirty turns of magnetic wire were wrapped through the current

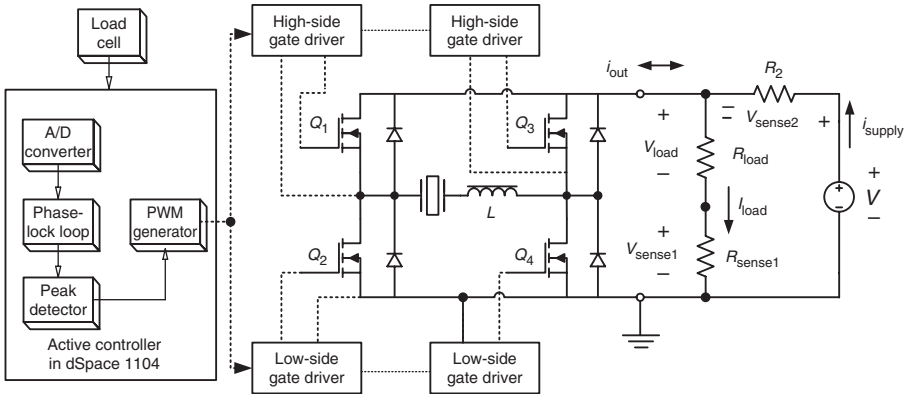

Figure 11. *Active energy harvesting circuit.*

probe to improve the resolution of the current measurement. These probes were connected to a Tektronics TDS 754D oscilloscope.

For the first series of tests a single-layer device was used. This device was mechanically excited so that it experienced an effective strain of 0.7%. The voltage across the device was controlled by the full-bridge inverter to transition between ±25 V. The lower switches of the inverter were pulse-width modulated at a switching frequency of 50 kHz and a duty cycle of ~5%. The resulting measured piezoelectric voltage and current are shown in Figure 12. It should be noted that the charging and discharging current of the device cannot be seen in this data, due to the sampling frequency of the oscilloscope and the high-frequency nature of the current during charging and discharging. Figure 13 shows the current through the device at a time scale corresponding to the pulse-width modulation of the lower MOSFETs. The gate-source voltage of the corresponding lower MOSFET is also shown (the MOSFET is 'on' when this voltage is 15 V, and is 'off' when this voltage is 0 V). Inspection of Figure 12 shows that the voltage and current waveforms tend to have the same sign, resulting in positive (i.e., harvested) power flow.

For the next series of experiments a four-layer PVDF device was used. The switching frequency of the inverter was changed to 5 kHz, and a duty cycle of 1% was applied to the low-side MOSFETs during the voltage transitions. The average harvested power was then determined by subtracting the power provided by the DC voltage source from the power dissipated by the DC load resistance R_{load}. It should be noted that, in these experiments, the power for the gate drive and control system is not included when calculating harvested energy. The power that flows from the gate driver circuitry to the inverter is only used to charge the gate capacitances of the MOSFETs, and so will not be added to the power harvested. Figure 14 shows the results of this harvested power as a function of the DC bus voltage for an effective mechanical strain of 0.81%. As predicted by theory, it is seen that an optimal bus voltage exists that maximizes the power harvested.

The performance of the active energy harvesting approach as a function of effective mechanical strain is shown in Figure 15, where it is compared to the power extracted by a passive diode rectifier circuit operating at its optimal output voltage, and to the resulting power from the diode rectifier circuit after being converted by a DC–DC converter to a desired output voltage of 1–2 V. For the active data, the bus voltage was manually

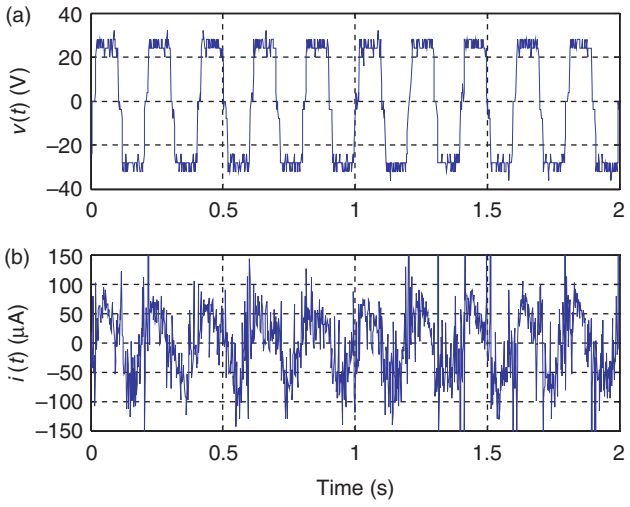

Figure 12. *Energy harvesting experiment with single-layer PVDF device excited mechanically at a frequency of 5 Hz and with an effective strain of 0.7%: (a) measured voltage across piezoelectric device; (b) measured current through piezoelectric device.*

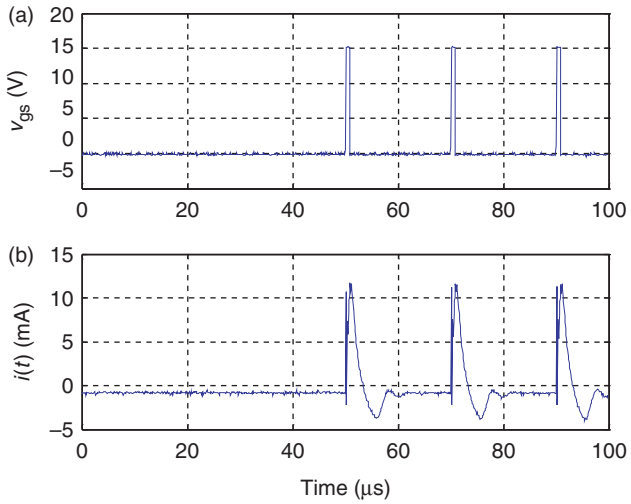

Figure 13. *Energy harvesting experiment with single-layer PVDF device excited mechanically at a frequency of 5Hz and with an effective strain of 0.7%: (a) gate-source voltage of lower MOSFET; (b) measured current through piezoelectric device.*

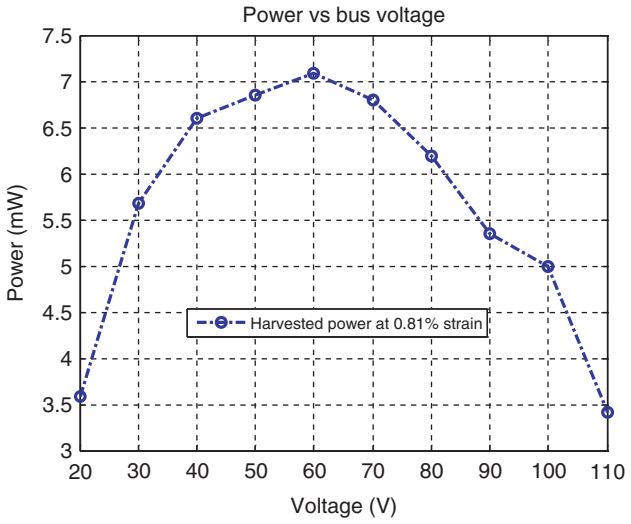

Figure 14. *Harvested electric power as function of DC bus voltage for mechanical excitation of 0.81% effective strain.*

adjusted to its optimal value. As can be seen in the figure, the maximum power harvested by the active approach is up to five times higher than that with the passive approach. Based upon the chart provided in Figure 8, this suggests the efficiency of the full-bridge inverter circuit is ~78%.

CONCLUSIONS AND FUTURE WORK

The evolution of energy harvesting from passive to active form can result in significantly higher performance. In this article, we attempt to establish a fundamental understanding of such a system. The power electronic efficiency was shown to be one of the most important limiting factors of active energy harvesting.

Experimentally, it is also demonstrated that active energy harvesting can greatly increase the harvested power for the same mechanical force input without modification of the piezoelectric device. Fundamentally, it is due to two effects of the active energy harvesting system. First, actively controlling the electrical boundary condition changes the mechanical boundary condition so that more mechanical energy is captured by the piezoelectric material. Second, active energy harvesting approach increases the effective electromechanical coupling of the system in the sense of converted energy to stored energy ratio.

The proposed energy harvesting technique, while similar in appearance and behavior to the SSHI technique, actually possesses some significant differences. One main distinction is that, with SSHI, power is transferred to the load only under transient conditions, whereas with the active approach discussed here the power flow associated with electromechanical energy conversion occurs at essentially all times. Another distinction is that the frequency of operation of the semi-conductor switch in SSHI is the same as that as the mechanical excitation, whereas in the proposed active approach the switching frequency of the transistors is much faster. This allows much greater control over the piezoelectric voltages and currents as opposed to SSHI. In particular, the peak current in the device can be controlled by the duty cycle of the transistors rather than through the circuit design. This allows the active approach to use a much smaller inductor than SSHI for a given peak current, for example. Lower peak currents can result in more efficient power transfer.

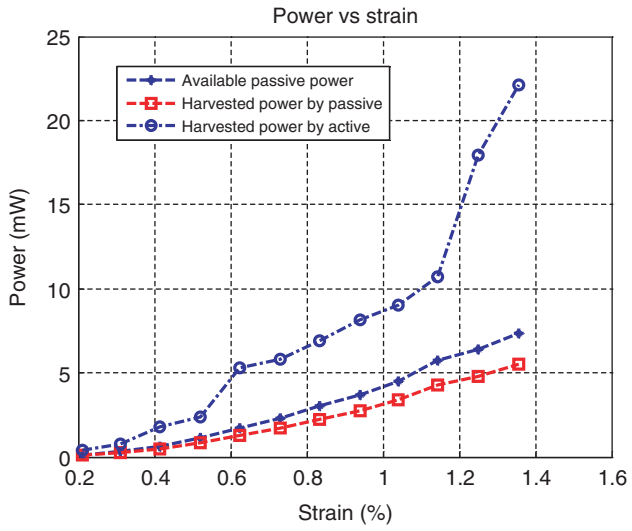

Figure 15. *Harvested electrical power as a function of effective mechanical strain, active approach compared to passive diode rectifier, and passive diode rectifier with DC/DC converter.*

An important feature of active energy harvesting is that the circuitry must be capable of bidirectional power flow. The circuit must also initially possess some energy to initiate active energy harvesting. This could be achieved through the use of a passive energy harvesting scheme, which could then revert to active energy harvesting after sufficient energy has been stored. In the case of the full-bridge converter, the body diodes of the power MOSFETs in this circuit could act as a full-bridge diode rectifier, thereby achieving passive energy harvesting.

For quick prototyping purposes, we used a digital-signal processor (DSP) to implement the controller in the active energy harvesting experiment. However, the controller implementation for the proposed approach can be quite simple. For example, in the case of voltage control a peak detector on the measured force could be used to trigger the voltage transition. This is similar to the controllers for other energy harvesting implementations, such as SSHI. Future work will involve the development of a standalone controller implementation.

In the experiments presented in this article, the power required to drive the MOSFET switches came from an external power source, and was not included in the energy harvesting calculations. This power is determined by the amount of charge that is placed onto the gate of the MOSFET during turn-off and removed during turn-on, which is determined by the size of the capacitances between the gate-source and gate-drain of the MOSFET. The size of these capacitances is determined by the dimensions of the MOSFET, which in turn are determined by the current and voltage ratings of the device. Therefore, the power required for switching the MOSFETs scales with the power output of the circuit, and a standalone circuit should be possible with sufficiently high efficiency. This can be seen through the inspection of the efficiencies of commercially available power electronic converters. Even at power levels in the milliwatt range, these converters can still achieve reasonably high efficiencies, including controller and gate-driver losses. Initial efforts in this area have suggested that the power consumed by controlling the

MOSFETs in the presented system can be on the order of 1 mW. Future work will involve the completion of the development of such a standalone circuit.

The embodiment of active energy harvesting shown here requires a fixed voltage 'source'. In a standalone circuit, these voltages could be established via rechargeable batteries, for example. Another approach would be to generate these voltages initially through passive energy harvesting techniques (when the MOSFETs of the full-bridge converter are all off the circuit becomes a full-bridge diode rectifier due to the body diodes of the MOSFETs), and then convert to active energy harvesting when the voltages have been established.

A simplified piezoelectric system, using a quasi-static model, is used in this analysis. The general conclusions, however, could be extended to a more complex dynamic system. Future work will involve investigations into this area.

APPENDIX

In the following we will use the constitutive relationships Equation (2) for piezoelectric material, and the energy is calculated by:

$$W = \int VI\,\mathrm{d}t = \int V\frac{\mathrm{d}Q}{\mathrm{d}t}\mathrm{d}t = \int V\,\mathrm{d}Q = \int C^F V\,\mathrm{d}V + \int \mathrm{d}V\,\mathrm{d}F. \quad (21)$$

Hence, power flows through the device due to a change in either electrode voltage or mechanical force. We consider the two cases discussed in 'Efficiency of Power Electronics' section.

1. In Case 1, where $V_{\min} > 0$, power flows into the device along paths 1–2 and 2–3; along path 1–2 the power flow is due to the change in mechanical force when the electrode voltage is $V_{\min}$, and along path 2–3 power flows into the device due to the charging of the electrode capacitance from $V_{\min}$ to $V_{\max}$. The net energy flow into the device is therefore given by:

$$W_{\text{in}} = d(F_{\max} - F_{\min})V_{\min} + \frac{1}{2}C^F\left(V_{\max}^2 - V_{\min}^2\right). \quad (22)$$

   Power flows out of the device along path 3–4 due to the change in force when the electrode voltage is $V_{\max}$, and along path 4–1 due to the discharging of the electrode capacitance. The net output energy along these paths is therefore:

$$W_{\text{out}} = d(F_{\max} - F_{\min})V_{\max} + \frac{1}{2}C^F\left(V_{\max}^2 - V_{\min}^2\right). \quad (23)$$

2. In Case 2, as $V_{\min} < 0$, the power flow along paths 1–2 and 3–4 are both out of the device (this is a key reason why Case 2 is preferable). As a result, the only power flow into the device is due to the charging of the electrode capacitance. This occurs as the electrode voltage changes from 0 V to either $V_{\min}$ or $V_{\max}$. The total energy flowing into the device under these conditions is therefore given by:

$$W_{\text{in}} = \frac{1}{2}C^F\left(V_{\min}^2 + V_{\max}^2\right). \quad (24)$$

The total energy output consists of the power flow due to the change in mechanical force along paths 1–2 and 3–4, and due to the discharging of the electrode voltage from both $V_{\min}$ and $V_{\max}$ to 0 V:

$$W_{\text{out}} = d(V_{\max} - V_{\min})(F_{\max} - F_{\min}) + \frac{1}{2}C^F\left(V_{\max}^2 + V_{\min}^2\right). \quad (25)$$

The net energy is therefore given by:

$$W_{\text{net}} = \eta W_{\text{out}} - \frac{1}{\eta}W_{\text{in}} = \eta d(V_{\max} - V_{\min})(F_{\max} - F_{\min}) - \frac{1}{2}C^F\left(\frac{1}{\eta} - \eta\right)\left(V_{\max}^2 + V_{\min}^2\right). \quad (26)$$

For a given voltage range $V_L = V_{\max} - V_{\min}$, and force range $F_L = F_{\max} - F_{\min}$, this energy is maximized by minimizing $(V_{\max}^2 + V_{\min}^2)$. It is straightforward to show that this occurs when $V_{\min} = -V_L/2$, $V_{\max} = V_L/2$. Under these conditions, the net energy harvested is given by:

$$W_{\text{net}} = \eta\, dV_L F_L - \frac{1}{4}C^F\left(\frac{1}{\eta} - \eta\right)V_L^2. \quad (27)$$

We can then determine the voltage range V_L that maximizes this expression by differentiating the expression with respect to V_L and setting the result to zero:

$$\frac{\partial W_{\text{net}}}{\partial V_L} = \eta\, dF_L - \frac{1}{2}C^F\left(\frac{1}{\eta} - \eta\right)V_L = 0. \quad (28)$$

Solving, we obtain:

$$V_L = 2\left(\frac{\eta^2}{1-\eta^2}\right)\frac{dF_L}{C^F} = 2\left(\frac{\eta^2}{1-\eta^2}\right)V_{\text{oc}}, \quad (29)$$

where V_{oc} is the open-circuit voltage of the device under peak-to-peak force F_L, and is defined as: $\mathrm{V_{oc}} = \mathrm{d}F_L/C^F$. The resulting maximum energy harvested is therefore given by:

$$W_{\max\ \text{ac}} = \left(\frac{\eta^3}{1-\eta^2}\right)C^F V_{\text{oc}}^2. \quad (30)$$

ACKNOWLEDGMENTS

The authors would like to thank Dr John Blottman and the Naval Undersea Warfare Center for their support of this work under Grant No. N66604-07-1-2678.

REFERENCES

Badel, A. 2005. "Efficiency Enhancement of a Piezoelectric Energy Harvesting Device in Pulsed Operation by Synchronous Charge Inversion," *Journal of Intelligent Material Systems and Structures*, 16(10):889–901.

Badel, A., Benayad, A., Lefeuvre, E., Lebrun, L., Richard, C. and Guyomar, D. 2006. "Single Crystals and Nonlinear Process for Outstanding Vibration-powered Electrical Generators," *IEEE Trans. Ultrason. Ferroelectr. Freq. Control*, 53(4):673–677.

Badel, A., Sebald, G., Guyomar, D., Lallart, M., Lefeuvre, E., Richard, C. and Qiu, J. 2006. "Piezoelectric Vibration Control by Synchronized Switching on Adaptive Voltage Sources: Towards Wideband Semi-active Damping," *Journal of the Acoustical Society of America*, 119(5):2815–2825.

Faiz, A., Guyomar, D., Petit, L. and Buttay, C. 2005. "Semi-passive Piezoelectric Noise Control in Transmission by Synchronized Switching Damping on Voltage Source," *Journal De Physique*. IV, 128:171–176.

Hagood, N.W. and Ghandi, K. 2003. "Electrical Power Extraction from Mechanical Disturbances," U.S. Patent, 6 580177.

IEEE Standard on Piezoelectricity, 29 Jan 1988.

Lefeuvre, E., Badel, A., Richard, C. and Guyomar, D. 2005. "Piezoelectric Energy Harvesting Device Optimization by Synchronous Electric Charge Extraction," *Journal of Intelligent Material Systems and Structures*, 16(10):865.

Liu, Y., Ren, K., Hofmann, H. and Zhang, Q.M. 2005. "Investigation of Electrostrictive Polymers for Energy Harvesting," *IEEE Transactions on Ultrasonics, Ferroelectrics, and Frequency Control*, 52(12):2411–2417.

Mohan, N., Undeland, T.M. and Robbins, W.P. 2003. *Power Electronics: Converters, Applications, and Design*, John Wiley & Sons, Inc., Hoboken, N.J.

Newnham, R.E., Skinner, D.P. and Cross, L.E. 1978. "Connectivity and Piezoelectric-pyroelectric Composites," *Mater. Res. Bull.*, 13:525–536.

Newnham, R.E. and Zhang, J. 2001. "Cymbal Transducer: A Review," In: *Proceedings of the 12th IEEE International Symposium on Applications of Ferroelectrics*, pp. 29–32.

Ottman, G.K., Hofmann, H.F., Bhatt, A.C. and Lesieutre, G.A. 2002. "Adaptive Piezoelectric Energy Harvesting Circuit for Wireless Remote Power Supply," *IEEE Transactions on Power Electronics*, 17(5):669–676.

Ottman, G.K., Hofmann, H.F. and Lesieutre, G.A. 2003. "Optimized Piezoelectric Energy Harvesting using Step-down Converter in Discontinuous Conduction Mode," *IEEE Transactions on Power Electronics*, 18(2):696–703.

Richard, C., Guyomar, D., Audigier, D. and Bassaler, H. 2000. "Enhanced Semi Passive Damping using Continuous Switching of a Piezoelectric Device on an Inductor," In: *Proceedings of SPIE - The International Society for Optical Engineering*, 3989: 288–299.

Smalser, P. 1997. "Power Transfer of Piezoelectric Generated Energy," U.S. Patent, 5 703 474.

Wang, Q.M., Du, X.H., Xu, B. and Cross, L.E. 1999. "Electromechanical Coupling and Output Efficiency of Piezoelectric Bending Actuator," *IEEE Trans. Ultrason., Ferroelect., Freq. Contr.*, 46(3):638–646.

Wang, Y., Ren, K.L. and Zhang, Q.M. 2007. "Direct Piezoelectric Response of Piezopolymer Polyvinylidene Fluoride under High Mechanical Strain and Stress," *Applied Physics Letters*, 91(22), pp. 222905-1-3.